# Atomic Force Microscopy-Based Molecular Recognition of a Fibrinogen Receptor on Human Erythrocytes

**Filomena A. Carvalho,[†] Simon Connell,[‡] Gabriel Miltenberger-Miltenyi,[†,§] Sónia Vale Pereira,[§] Alice Tavares,[⊥] Robert A. S. Ariëns,[∥] and Nuno C. Santos[†,*]**

[†]Instituto de Medicina Molecular, Faculdade de Medicina da Universidade de Lisboa, 1649-028 Lisboa, Portugal, [‡]School of Physics and Astronomy, University of Leeds, LS2 9JT Leeds, United Kingdom, [§]GenoMed Diagnósticos de Medicina Molecular, 1649-028 Lisboa, Portugal, [⊥]Serviço de Imuno-Hemoterapia, Hospital de Santa Maria, Centro Hospitalar Lisboa Norte, 1649-028 Lisboa, Portugal, and [∥]Division of Cardiovascular and Diabetes Research, Leeds Institute for Genetics, Health and Therapeutics, University of Leeds, LS2 9JT Leeds, United Kingdom

**ABSTRACT** The established hypothesis for the increase on erythrocyte aggregation associated with a higher incidence of cardiovascular pathologies is based on an increase on plasma adhesion proteins concentration, particularly fibrinogen. Fibrinogen-induced erythrocyte aggregation has been considered to be caused by its nonspecific binding to erythrocyte membranes. In contrast, platelets are known to have a fibrinogen integrin receptor expressed on the membrane surface (the membrane glycoprotein complex $\alpha_{IIb}\beta_3$). We demonstrate, by force spectroscopy measurements using an atomic force microscope (AFM), the existence of a single molecule interaction between fibrinogen and an unknown receptor on the erythrocyte membrane, with a lower but comparable affinity relative to platelet binding (average fibrinogen—erythrocyte and —platelet average (un)binding forces were 79 and 97 pN, respectively). This receptor is not as strongly influenced by calcium and eptifibatide (an $\alpha_{IIb}\beta_3$ specific inhibitor) as the platelet receptor. However, its inhibition by eptifibatide indicates that it is an $\alpha_{IIb}\beta_3$-related integrin. Results obtained for a Glanzmann thrombastenia (a rare hereditary bleeding disease caused by $\alpha_{IIb}\beta_3$ deficiency) patient show (for the first time) an impaired fibrinogen—erythrocyte binding. Correlation with genetic sequencing data demonstrates that one of the units of the fibrinogen receptor on erythrocytes is a product of the expression of the $\beta_3$ gene, found to be mutated in this patient. This work demonstrates and validates the applicability of AFM-based force spectroscopy as a highly sensitive, rapid and low operation cost nanotool for the diagnostic of genetic mutations resulting in hematological diseases, with an unbiased functional evaluation of their severity.

**KEYWORDS:** fibrinogen · erythrocyte · platelet · atomic force microscopy · Glanzmann thrombasthenia · force spectroscopy

The use of nanotechnologies for medical applications raises high expectations regarding diagnosis, drug delivery, gene therapy and tissue engineering. There is an increasing number of reports using AFM as a nanodiagnostic tool with patient cells. Cross *et al.* showed that cancer cells from patients have a significant decrease of their cell stiffness, when compared with healthy cells.[1,2] Another report used AFM to detect early stages of cartilage degeneration on osteoarthritis that could not be detected by the most common available techniques. Besides its direct relevance on the identification of the fibrinogen receptor on erythrocytes (red blood cells) and of a pharmacological strategy to inhibit it, our present work is also a demonstration of the applicability and validation of the AFM-based force spectroscopy technique as a highly sensitive, rapid and low operation cost nanotool for the diagnostic and unbiased functional evaluation of the severity of hematological diseases arising from genetic mutations, such as Glanzmann thombasthenia.

To stop a bleeding, blood clotting occurs when fibrinogen, one of the more abundant plasma proteins, polymerizes, forming a fibrin network that entraps erythrocytes and platelets to form a clot. Human fibrinogen is a 340 kDa glycoprotein, consisting of two symmetric subunits, each one containing three nonidentical polypeptide chains (Aα, Bβ and γ).[3] These subunits are grouped into three major structural regions: two D-domains and one central E-domain. Integrin receptors, expressed on the platelets surface, play a critical role on blood clotting regulation.[4,5] Fibrinogen contains three potential integrin binding sites: two RGD (arginine-glycine-aspartic acid) amino acid sequences within the Aα chain and a 12 amino acids (dodecapeptide) sequence on the γ chain but can also interact with cells through nonintegrin receptors.[3] The membrane glycoprotein complex $\alpha_{IIb}\beta_3$ is the well characterized platelets integrin receptor for fibrinogen.[5] Ligand binding to this integrin heterodimer involves specific regions of the amino-terminal portions of both $\alpha_{IIb}$ and $\beta_3$ units. Fibrinogen binding is enabled only after activation by the association of four calcium ions to the integrin.[4,6]

*Address correspondence to nsantos@fm.ul.pt.

Received for review May 4, 2010 and accepted July 14, 2010.

**Published online July 23, 2010.**
10.1021/nn1009648

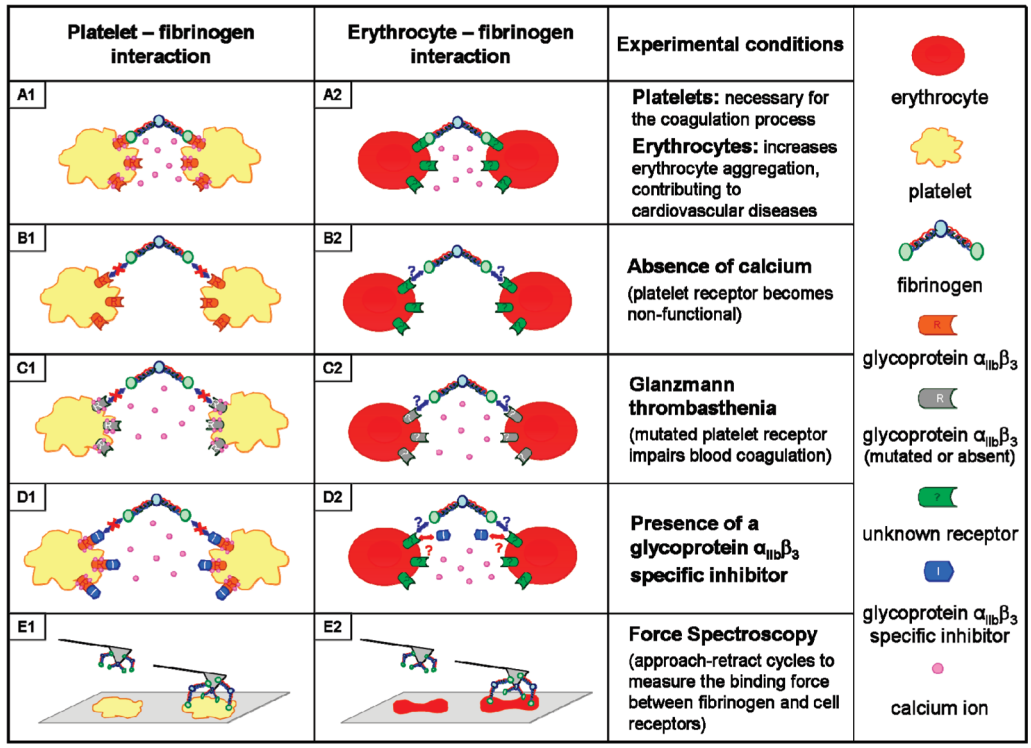


**Figure 1. Diagram illustrating platelet−fibrinogen and erythrocyte−fibrinogen interactions at different experimental conditions. (A) Physiological conditions. During the coagulation process, platelets and glycoprotein $\alpha_{IIb}\beta_3$ receptor are activated, in the presence of calcium ions. Fibrinogen molecules binds to platelets, bridging them to form the blood clot and to stop bleeding (A1). Fibrinogen binds to an unknown receptor on erythrocytes, leading to an increase of erythrocyte aggregation and contributing to cardiovascular diseases (A2). (B) Absence of calcium. In the absence of calcium, glycoprotein $\alpha_{IIb}\beta_3$ receptor is inactivated, unabling its binding to fibrinogen (B1). The identical situation on erythrocytes was evaluated in this study (B2). (C) Glanzmann thrombasthenia. Glanzmann thrombastenia patients have a quantitative (absent) or qualitative (mutated) $\alpha_{IIb}\beta_3$ platelet receptor deficiency; therefore, the binding to fibrinogen does not occur or is diminished, even in the presence of calcium (C1). The binding between fibrinogen and the erythrocyte unknown receptor on GT patients was also investigated (C2). (D) Presence of a glycoprotein $\alpha_{IIb}\beta_3$ specific inhibitor eptifibatide. In the presence of this inhibitor and with calcium ions, the binding of fibrinogen to platelets decrease or is abolished (D1). The effect of this inhibitor on the unknown erythrocyte receptor was also measured (D2). (E) AFM-based force spectroscopy measurements. Approach and retract cycles were performed to measure the (un)biding force between fibrinogen (covalently attached to the AFM tip) and the receptors on the surface of the blood cells, deposited on a glass slide (E1 and E2).**

Antiplatelet therapies can target individual receptor-linked activation pathways. Glycoprotein $\alpha_{IIb}\beta_3$ inhibitors block the binding of fibrinogen to the glycoprotein $\alpha_{IIb}\beta_3$ receptors. Eptifibatide is a cyclic heptapeptide that inhibits specifically and reversibly the binding of fibrinogen to the glycoprotein $\alpha_{IIb}\beta_3$ receptor in platelets. It is derived from the structure of an anticoagulant peptide found in the venom of the southeastern pigmy rattlesnake (*Sistrurus m. barbouri*).[7] It contains a KGD (lysine-glycine-aspartic acid) amino acid sequence, identical to that in the γ-chains of fibrinogen.[8] These molecules are clinically used as anti-integrin therapies for the treatment of pathologic increases on platelet aggregation.

In addition to its important role in mediating platelet adhesion, $\alpha_{IIb}\beta_3$ is essential for platelet aggregation upon blood clotting, as demonstrated in Glanzmann thrombasthenia (GT) patients.[3,9] This is a rare hereditary bleeding syndrome caused by a quantitative or qualitative $\alpha_{IIb}\beta_3$ deficiency.[10] The platelets from individuals with this defective receptor fail to aggregate, as this glycoprotein mediates the binding to fibrinogen.[10,11]

Increased fibrinogen concentration[12] and erythrocyte aggregation[13] are factors that significantly increase the risk of cardiovascular and cerebrovascular diseases. The prevailing hypothesis for the mechanism of fibrinogen-induced erythrocyte hyperaggregation has been that it is caused by a nonspecific binding mechanism.[12] However, the published data on the changes in erythrocyte aggregation during hypertension points to the possible existence of other mechanism(s).[14]

At the moment, only a few studies were done using atomic force microscopy (AFM) based force spectroscopy to study related systems, but none of them studied the interaction of the entire fibrinogen molecule and its specific receptors on blood cells. In 2003, Lee and Marchant studied the binding between the RGD peptide and the receptor on platelet and between the fibrinogen dodecapeptide and the receptor on platelets.[6] Litvinov *et al.* also reported on the fibrinogen binding to the isolated glycoprotein $\alpha_{IIb}\beta_3$.[15]

In the present work, we evaluated the existence of a specific binding between fibrinogen and an unknown receptor on the human erythrocyte membrane. For the sake of comparison, an equivalent study was conducted with human platelets. We performed force spectroscopy studies with cells from healthy donors and a patient with Glanzmann thrombasthenia. Knowing that the activation of the integrin $\alpha_{IIb}\beta_3$ complex is dependent on the presence of calcium ions, we performed equivalent force spectroscopy experiments in the absence of calcium. We also conducted similar studies in the presence of the specific inhibitor of $\alpha_{IIb}\beta_3$ platelet receptor eptifibatide. All these results allow us to characterize the erythrocyte receptor for fibrinogen and compare it with the glycoprotein $\alpha_{IIb}\beta_3$ platelet receptor. Figure 1 presents a schematic diagram illustrating the interactions between blood cells membrane receptors and the fibrinogen molecule at all the different experimental conditions tested in the present work. Our data indicate that there is a specific binding between fibrinogen and the erythrocyte membrane, with a lower but comparable affinity to the platelets binding. This interaction is mediated by an erythrocyte's integrin $\alpha_{IIb}\beta_3$-like receptor, in which one of its units is expressed by the same gene as platelet's $\beta_3$ unit.

## RESULTS

**AFM Scanning Images of Human Blood Cells.** Platelets collected from healthy human donors were scanned by AFM, showing different activation states (spiky, partially spread and fully spread). Figure 2A,B show, respectively, the height and error signal images of spiky morphology of platelets isolated from human blood in the presence of $CaCl_2$. Imaging reveals that human platelets have 3−5 μm of diameter, which is the expected size for these cells. The height of deposited platelets ranged between 350 and 650 nm, depending on their activation state. Platelets with irregular surface and extended pseudopods about 1−2 μm long can also be seen (Figure 2B).

Human erythrocytes AFM image (Figure 2C,D; height and error signal image, respectively) revealed the common disk shape of human erythrocytes, with 8−10 μm of diameter and a height of approximately 1−1.5 μm. In Figure 2C, the biconcave disk shape of erythrocytes can easily be seen.

Both cell types showed good adherence to glass slides coated with poly-L-lysine (a positively charged polymer).

**Force Spectroscopy of Fibrinogen−Platelet and Fibrinogen−Erythrocyte Interactions.** When a fibrinogen-functionalized tip contacts the cells surface in buffer with calcium, the force curves show well-defined and measurable adhesion forces. The frequency of adhesion-rupture events achieved from the platelet-fibrinogen system was 22%. For the erythrocyte-fibrinogen system this percentage was only slightly lower (17%). From these adhesion events, approximately 75% were of single rupture events and the remaining 25% were from double or multiple steps binding events, for the two systems studied.

The distribution of rupture forces between fibrinogen-functionalized tip and erythrocyte or platelet surface ranged from several piconewtons to 1 nN, with the probability of forces above 500 pN being very low (<5%) (Figure 3B). Rupture force values are defined as the force necessary to break the bond between one molecule of fibrinogen and one cell receptor, which is characterized by the instantaneous jumps in force seen in Figure 3A. Rupture length values are defined as the distance between the cell-AFM tip contact point (defined as the zero point value at the force curve plot, Figure 3A) and the height value at the moment when the cell receptor-fibrinogen bond breaks.

Figure 3B shows typical histograms of rupture force events for the fibrinogen−erythrocyte and fibrinogen−platelet systems, in the presence of $Ca^{2+}$ 1 mM. Experimental data were fitted with Gaussian curves to obtain the average rupture force for a single fibrinogen-cell receptor binding, yielding values of 79 ± 3 pN for erythrocytes and 97 ± 2 pN for platelets. These values are statistically different ($P < 0.001$; unpaired samples *t*-test). Thus, fibrinogen−erythrocyte binding has a lower but comparable force than the one between fibrinogen and its platelet specific receptor. The two peaks observed on both histograms with forces above 150 pN are from multiple binding events between different fibrinogen molecules and its cell receptors.

The length of the rupture adhesion events was also analyzed by fitting the histograms with Gaussian curves. Two distinct peaks were obtained for each protein-cell receptor, which were 145 and 245 nm for erythrocytes and 120 and 250 nm for platelets (Figure 3C). It should be borne in mind that this rupture length values are influenced by the stretching of the elastic platelet or erythrocyte surface and, eventually, by the unfolding of the polypeptide chains of the fibrinogen molecules.[16] The two coiled-coil regions (Aα, Bβ and γ-chains) in fibrinogen are each 111 amino-acid residues long, which, when fully unfolded, are expected to be 40 nm long. In contrast, the C-terminal γ-chain, consisting of 215 amino-acid residues, has 77 nm.[9,17]

**Validation Experiments.** We performed identical force spectroscopy experiments with cells isolated from one patient with Glanzmann thrombasthenia, resulting from a mutation on the fibrinogen receptor in platelets, to have an ideal negative control for the studied system, and to confirm that what we are measuring is in fact the binding forces between fibrinogen molecules and its specific platelet receptor (*vd.* Genetic analysis).

This GT patient presented a drastic decrease on the frequency of binding/unbinding events. The average

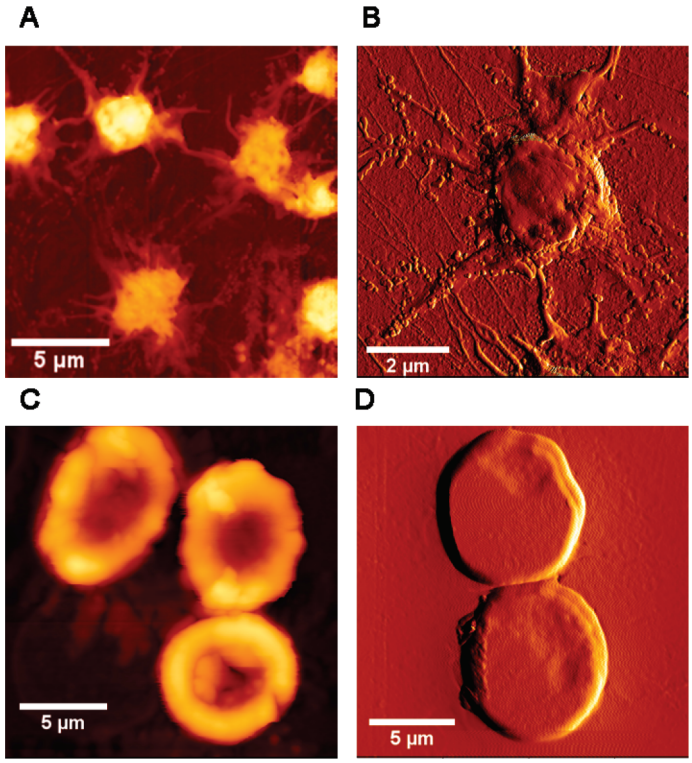


**Figure 2. Air tapping-mode AFM images of human platelets (A,B) and human erythrocytes (C,D) from healthy donors, deposited on poly-L-lysine coated glass slides. (A,C) Height images; (B,D) error signal images. AFM images of typical circular, biconcave erythrocytes and spiky human blood platelets.**

force rupture value obtained for the fibrinogen-platelet system was 38 ± 0.1 pN (mean ± SE; Figure 4). This significant decrease of the force value for fibrinogen-$\alpha_{IIb}\beta_3$ platelet receptor confirms the specificity of these experiments. Interestingly, a similar decrease on the efficiency of the fibrinogen-receptor interaction was observed for the erythrocytes of this patient, with a decrease on the average force rupture value to 37 ± 0.4 pN (mean ± SE). This is the first assessment of the interaction of fibrinogen with erythrocytes in a GT patient and the first proof of its impairment.

No background adhesion force between an unmodified silicon nitride tip and the platelet or erythrocyte surface was detected (Figure 3A). When a nonfunctionalized tip contacts with poly-L-lysine-coated glass slides, or a fibrinogen-functionalized tip contacts with a clean noncoated glass surface, only weak interactions were detected. Adhesive interactions were not detected during the approach to the cell surface, but only on tip retraction. Interactions between a fibrinogen-functionalized tip and a poly-L-lysine coated glass slide were also detected but in a lower range than the fibrinogen-erythrocyte and fibrinogen-platelet binding (<40 pN). This force rupture histogram could not be fitted with the Gaussian model (data not shown).

**Effect of the Absence of Calcium.** As a first step for the characterization of the fibrinogen specific binding to erythrocytes, we tested its $Ca^{2+}$-dependence. This dependence has been reported for the fibrinogen-platelet binding.[18] Therefore, the same evaluation on platelets constitutes a further experimental control. Force spectroscopy experiments were done without including $CaCl_2$ in the BSGC buffer, and adding instead two different concentrations (1 mM and 4 mM) of ethylenediamine tetraacetic acid (EDTA) to chelate any trace amount of calcium free in solution. From the force rupture histograms shown on Figure 5, it can be seen that in the presence of EDTA there is only one Gaussian force peak for each studied systems. For the erythrocyte-fibrinogen system, the force rupture value was 61 ± 0.9 pN in the presence of EDTA 1 mM and 35 ± 6.7 pN for EDTA 4 mM (Figure 5A; both statistically different from the samples with $Ca^{2+}$; $P < 0.001$). The percentage of rupture events also decreases (for EDTA 4 mM, ~20% less than in the presence of calcium). For the binding between fibrinogen and its platelet receptor, the absence of calcium resulted in a significant decrease on the percentage of rupture events (for EDTA 4 mM, ~55% less than in the presence of calcium) and on the force rupture values, which decreased to 43 ± 0.8 pN in the presence of EDTA 1 mM and 30 ± 0.2 pN for EDTA 4 mM (Figure 5B; both statistically different from the samples with $Ca^{2+}$; $P < 0.001$). In fact, in the absence of calcium there is a stronger fibrinogen binding to erythrocytes than to platelets ($P < 0.001$ for EDTA 1 mM; for EDTA 4 mM the variation was not statistically significant, $P > 0.05$).

**Effect of the Presence of Eptifibatide.** To evaluate the similarity between the erythrocyte receptor for fibrinogen and the glycoprotein $\alpha_{IIb}\beta_3$ platelet receptor, force spectroscopy studies were done in the presence and absence of eptifibatide, a specific inhibitor of the platelet receptor. As a third control or proof of concept for the present experimental approach, the same evaluation was conducted with platelets.

As expected, results revealed that there are significant decreases on the percentage of rupture events and on the force rupture values of the fibrinogen−platelet system for all the eptifibatide concentrations (Figure 6B). Concentrations of 3.4, 8.5 and 17 μg/mL yielded binding/unbinding frequencies 42%, 54% and 80% lower than those obtained without eptifibatide, respectively. The force rupture values decrease considerably, to values between 32 and 45 pN, for all the eptifibatide concentrations studied (Figure 6B).

For the erythrocyte−fibrinogen system, in Figure 6A we observe that the same levels of inhibition attained with platelets are also reached, but only at the highest tested concentration. The average force rupture value in the presence of eptifibatide 3.4 μg/mL was 74 pN, 47 pN with eptifibatide 8.5 μg/mL and 32 pN with eptifibatide 17 μg/mL. The frequency of the binding/unbinding events decreases approximately 15% for the two lower eptifibatide concentrations and 65% for eptifibatide 17 μg/mL. The binding between erythrocytes

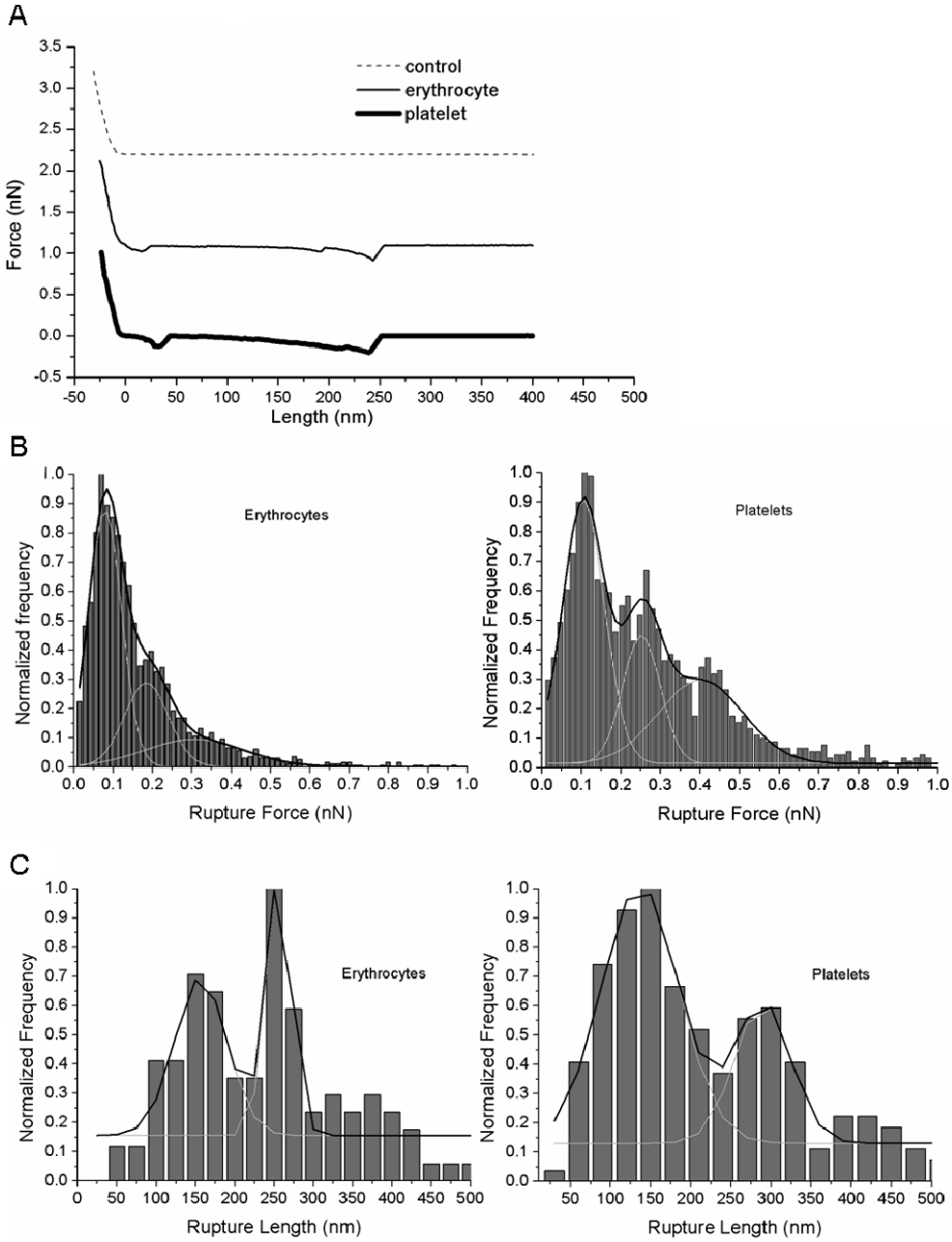


**Figure 3. Force spectroscopy results from healthy human blood donors in the presence of $Ca^{2+}$ 1 mM. (A) Typical force−extension curves of a control experiment of unmodified silicon nitride tip and the platelet/erythrocyte surface (---), where background adhesion forces were undetectable; a single fibrinogen−erythrocyte unbinding event (—); and a single fibrinogen−platelet receptor unbinding event (bold —). (B) Rupture-force histograms from about 8000 single event-force measurements for the fibrinogen−erythrocyte and fibrinogen−platelet systems. Measurements were done with an applied force of 1 nN, pulling speed of 2 μm/s and at a loading rate of 4 nN/s. (C) Rupture-length histograms from the same experimental curves referred in (B).**

and fibrinogen is influenced by the presence of eptifibatide, but not as significantly as for the fibrinogen−platelet binding.

The summary of the individual average rupture forces values obtained for the previously described different experimental conditions are summarized on Table 1.

**Single-Molecule Dynamic Force Spectroscopy.** To extract kinetic bond rupture parameters, using the Bell, Evans and Ritchie model,[19,20] experimental retraction velocities were varied between 0.5 and 16 μm/s. The contact time between the tip and the cell surface was approximately 1 μs. Loading rates were calculated for single adhesion events as a product of the effective spring constant with the retraction velocities. The effective spring constant was calculated from the slope of the force vs distance plot prior to the rupture. For the given retraction velocities, the corresponding effective loading rates are between 1 and 32 nN/s.

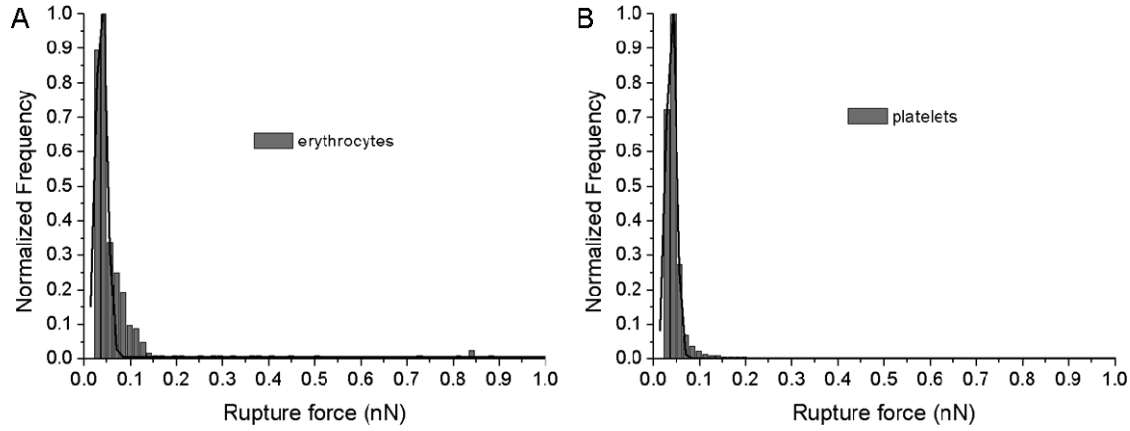


**Figure 4. Force rupture histograms from blood cells isolated from a Glanzmann thrombasthenia patient. (A) Fibrinogen−erythrocyte and (B) fibrinogen−platelet interactions.**

Under an AFM dynamic force spectrum for protein−ligand unbinding, the variation of the most probable unbinding force, $F$, with the natural logarithm of the loading rate, $r_f$, is a straight line in each regime of the spectrum, as set by the projected location of the potential barrier, $x_u$, along the direction of the force. Thus, mean values of the single rupture force and of the effective loading rate were used to construct a dynamic force spectrum (DFS), and the experimental data points in this graph were fitted to:

$$F = a \times \ln r_f + b \quad (1)$$

with $a = (k_B T)/(x_u)$ and $b = a \times \ln((1)/(a \times k_{off}))$, where $k_B$ is the Boltzmann constant, T the absolute temperature and $k_{off}$ the unstressed dissociation rate ($1/k_{off}$ is the bond lifetime). Equation 1 was applied to the fibrinogen-platelet receptor and fibrinogen-erythrocyte receptor systems, and the kinetic bond rupture parameters[21] calculated. The spectrum for a single-sharp energy barrier, where the logarithmic intercept can be used to obtain the activation energy barrier height, $E$, gives an estimate for the microscopic diffusion time such that:

$$\frac{E}{k_B T} \approx -\ln r_{f,F=0} + \ln a \quad (2)$$

From the record of the dependence of the rupture forces on the loading rate we can calculate the bond-specific parameters: $k_{off}$, the unstressed dissociation rate, $x_u$, the width of the potential barrier, and $1/k_{off}$, the bond lifetime. Increasing the loading rate, the average rupture force values increased from 72 to 105 pN for the platelet receptor-fibrinogen, and from 59 to 82 pN for the erythrocyte−fibrinogen system (Figure 7).

Plotting the mean rupture force vs the natural logarithm of each respective loading rate, the dynamic force spectrum for each studied system was obtained. The linearization of the dynamic force spectrum for both systems showed a sequence of two sharp activation energy barriers. Applying the Bell, Evans and Ritchie model (*vd.* eqs 1 and 2) to each linear regression equa-

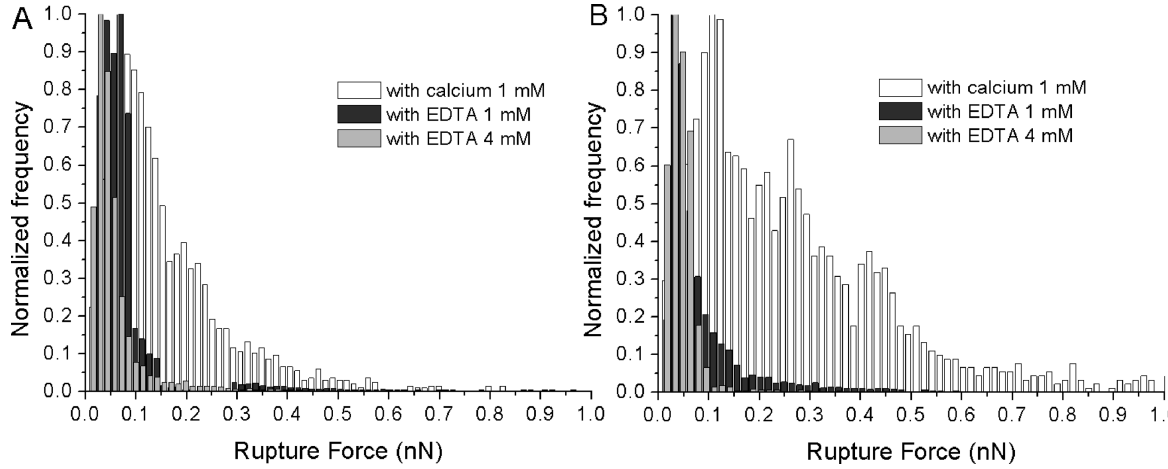


**Figure 5. Effect of the absence of calcium on fibrinogen-blood cells binding. Decrease in fibrinogen specific binding to human erythrocytes and platelets with the increase of $Ca^{2+}$ sequestring by the presence of different EDTA concentrations (1 mM and 4 mM). Force rupture histograms peaks obtained after choosing the best rupture force scale bin and fitting the (A) fibrinogen−erythrocyte and (B) fibrinogen−platelet rupture-fore histogram with the Gaussian model. Values of force rupture are presented as mean ± standard error (SE).**

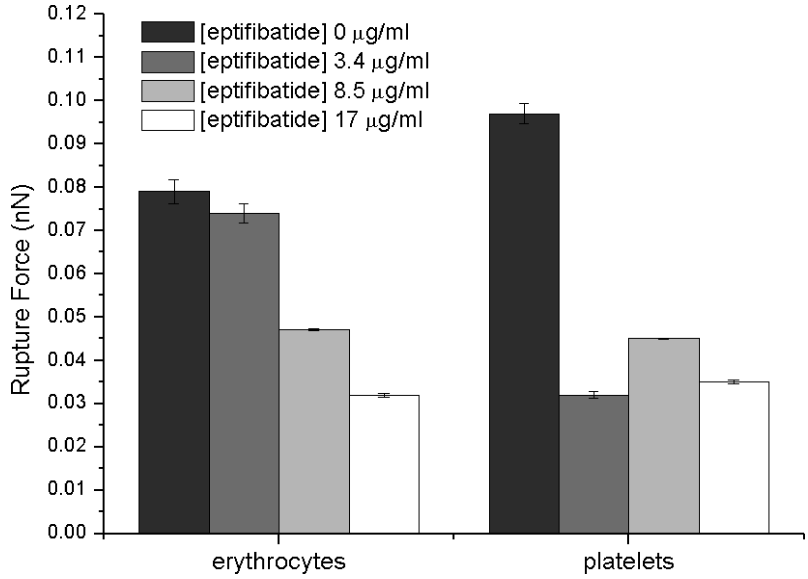


**Figure 6. Eptifibatide effect on fibrinogen-blood cells binding. Inhibition of (A) fibrinogen−erythrocyte and (B) fibrinogen−platelet binding by different concentrations of eptifibatide. Values of the average rupture forces (mean ± SE) obtained from the maximum value of the first Gaussian-fitted peak of the force histograms.**

tion, the different values of $E$, $k_{off}$, $1/k_{off}$ and $x_u$ were obtained (Table 2).

Our results for the erythrocyte−fibrinogen and platelet−fibrinogen systems are in accordance with the suggested biphasic logarithmic dependence for protein-receptor pairs.[21] Both systems have a primary regime with similar dissociation rate constants and energy barriers, but the binding between erythrocyte and fibrinogen have a bond lifetime of ~44 s, which is higher than the fibrinogen−platelet interaction bond lifetime. Moreover, the effective bond length of the potential barrier of the binding between fibrinogen and erythrocytes is 2.5 times higher than the one with platelets. On the second regime of the dynamic force spectroscopy chart, the results were totally different; resulting of the high loading rates applied on the force spectroscopy experiments. In this part, we could conclude that the binding between fibrinogen and platelets is much more stable than the one with erythrocytes, as it can be noticed on the considerably longer lifetime, shorter bond length and favorable energy barrier. On the last part of the linearization, the interaction between fibrinogen and erythrocytes only occurs for a few milliseconds, which corroborate the higher difficulty of the observation of this interaction *in vivo*.[22]

**Genetic Characterization of the Mutation for the Glanzmann Thrombasthenia Patient.** For the patient with Glanzmann thrombasthenia, we found a homozygous cytosine to thymine nucleotide change in the third coding exon of the *ITGB3* gene (c.262C > T), resulting in an arginine-to-stop codon substitution at codon 62 (p.R62X). In parallel, we did not find any mutations in the *ITGA2B* gene. The p.R62X mutation in *ITGB3* was already described in the literature as a pathogenic change associated to Glanzmann thrombasthenia.[23]

## DISCUSSION

We evaluated the possible existence of a specific fibrinogen receptor on erythrocyte membrane, using the tip of the AFM (derivatized with fibrinogen) as a nanotool for force spectroscopy measurements. From the results we can conclude that there is an unknown erythrocyte membrane receptor that specifically binds to fibrinogen with an average force of 79 ± 3 pN. This study was conducted in parallel with the evaluation of the already known, but never studied before by force

**TABLE 1. Average Force Rupture Values Obtained for the Fibrinogen−Platelet and Fibrinogen−Erythrocyte Systems at the Different Studied Conditions[a]**

| experimental conditions | erythrocyte receptor−fibrinogen rupture force (pN) | platelet receptor−fibrinogen rupture force (pN) |
|---|---|---|
| Presence of calcium $Ca^{2+}$ 1 mM | 79 ± 3.0 | 97 ± 2.0 |
| Absence of calcium | | 43 ± 0.8 |
| EDTA 1 mM | 61 ± 0.9 | 30 ± 0.2 |
| EDTA 4 mM | 35 ± 6.7 | |
| Presence of Eptifibatide | | |
| Eptifibatide 3.4 μg/mL | 74 ± 2.5 | 32 ± 0.8 |
| Eptifibatide 17 μg/mL | 32 ± 0.2 | 35 ± 0.4 |
| Glanzmann thrombasthenia patient | 37 ± 0.4 | 38 ± 0.1 |

[a]Values are presented as mean ± SE.

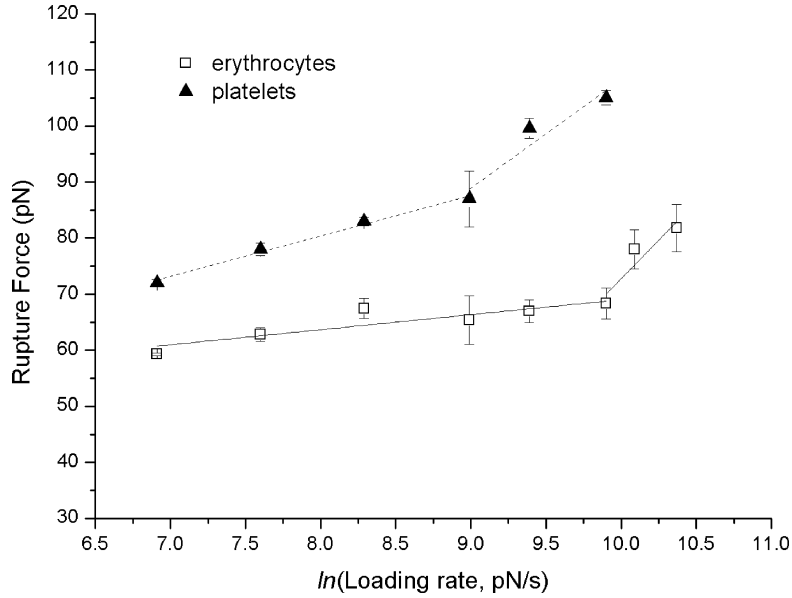


**Figure 7. Dynamic force spectra of fibrinogen-erythrocyte (□; solid line) and fibrinogen-platelet (▲; dashed line) (un)binding. Experimental values of the force ruptures dependence on the loading-rate, and theoretical fits obtained applying the Bell, Evans and Ritchie model to the two regimes.**

spectroscopy, specific interaction between fibrinogen and the glycoprotein $\alpha_{IIb}\beta_3$ receptor in platelets. An average force of 97 ± 2 pN was obtained for the rupture of the binding between fibrinogen and its platelet receptor. The erythrocyte−fibrinogen system has a lower rupture force than the determined for platelets; thus, as expected, we can conclude that fibrinogen has lower affinity for erythrocytes than for platelets. However, the proximity of the rupture force and binding frequency values obtained for both systems show an unexpected quantitative proximity between fibrinogen−erythrocyte and fibrinogen−platelet binding.

The rupture force value obtained for the fibrinogen−glycoprotein $\alpha_{IIb}\beta_3$ platelet receptor system (97 pN) are in accordance with other authors, who reported a rupture force value of 93 pN for the binding between the RGD peptide and the receptor on platelets and a value of 96.8 pN between the dodecapeptide and the receptor on platelets.[6] Litvinov *et al.* also reported a strong fibrinogen binding to the isolated glycoprotein $\alpha_{IIb}\beta_3$, with rupture forces peaking at 80−90 pN.[15] They also reported a typical force histogram, omitting values below 10 pN, containing two regimes of weak-moderate and strong binding, corresponding to 20−60 pN and 60−130 pN, respectively. The two-component fit used to quantify the force distributions and to compare $\alpha_{IIb}\beta_3$ receptor−fibrinogen interactions registered under different experimental conditions could also be applied to our data.

An increased erythrocyte aggregation is associated with a higher incidence of vascular pathgologies.[13] This erythrocyte hyperaggregation can result from increased plasma fibrinogen concentrations.[12] Until now, only a few reports were published describing a possible specific interaction between erythrocytes and fibrinogen[12,18,24] based on different experimental approaches. Lominadze *et al.* found that labeled fibrinogen binds rat erythrocyte membranes with a dissociation constant, $K_d$, of 1.3 μM, also estimating that the membrane of each erythrocyte has about 2000 fibrinogen binding sites[18] Rampling, also using labeled fibrinogen, estimated that *in vivo* 2% of fibrinogen circulates associated to erythrocytes, and that at normal fibrinogen concentrations (3 g/L) 20 000 molecules bind to each cell.[24] Comparing these two values with the reported $0.5-1 \times 10^5$ $\alpha_{IIb}\beta_3$ glycoproteins per platelet,[6] the number of specific receptors for fibrinogen per cell on erythrocytes is 5−50 times lower than on platelets. Rampling[24] and Maeda *et al.*[12] proposed the possible lo-

**TABLE 2. Kinetic Bond Rupture Parameters Calculated from the Linearization of the Dynamic Force Spectra for the Fibrinogen−Platelet and Fibrinogen−Erythrocyte Systems**

| cell receptor−fibrinogen | energy barrier ($k_BT$) | dissociation rate ($s^{-1}$) | bond lifetime (s) | barrier width (Å) |
|---|---|---|---|---|
| erythrocyte | | | | |
| 1st regime | 3.8 | 0.023 | 43.5 | 1.74 |
| 2nd regime | − 4.1 | 60.9 | 0.016 | 1.23 |
| platelet | | | | |
| 1st regime | 3.4 | 0.034 | 29.4 | 0.72 |
| 2nd regime | 3.7 | 0.026 | 38.5 | 0.17 |

cation of the erythrocyte-binding site in fibrinogen molecule to be in the Aα chain. Maeda *et al.* also proposed a model for the possible location of the binding regions on fibrinogen and how it affects the erythrocyte aggregation and flexibility. They estimated two different fibrinogen binding regions, which fit well with the hypothesis that erythrocyte aggregates are due to intermembrane cross-linking, that is, that the two binding sites on the fibrinogen molecule bind to different erythrocytes, bridging them.[12]

As for the previous reports on the fibrinogen−erythrocyte interaction, we have also evaluated this system by other experimental methodologies (unpublished data); however, as observed in previous studies, conventional methods are able to show that the fibrinogen-erythrocyte interaction exists, but fail on further characterizing it. We believe that this is a result of the transient character of the fibrinogen-erythrocyte interaction, which can be properly studied by force spectroscopy, but limits the details that are possible to assess by flow cytometry, for instance. This transient interaction cannot lead to clot formation, but is able to increase erythrocyte aggregation, increasing cardiovascular risk. The bond rupture kinetic parameters calculated from the Dynamic Force Spectra (*vd.* Table 2) show that the lifetime of the fibrinogen-erythrocyte bond is, in some situations, only 0.04% of the lifetime of the fibrinogen-platelet binding, pointing out why force spectroscopy is a specially appropriate methodology to study this interaction.

Force spectroscopy reveals to be a good biophysical method to determine the interaction forces between fibrinogen and human blood cells. At variance with other methodologies, the process of cell isolation is not an issue with this technique because the measurements are conducted at the single-cell level. After isolating the erythrocytes, the fibrinogen interactions are measured on the top of a single erythrocyte at a time, while it can be optically imaged in real-time, assuring that it is not a platelet or any other type of cell.

The coupling of biomolecules, such as fibrinogen, to tips has already proven to be important for measuring both inter and intramolecular forces with subnanonewton resolution.[25−27] Although the use of nonspecific adsorption allows the detection of discrete forces, the measurement of the interaction force between covalently bonded molecules permits the molecules to be firmly attached to the tip, in order not to be removed during the pulling of a ligand−receptor complex. In our study, the use of glutaraldehyde as a flexible cross-linker to covalently couple fibrinogen to the tip gives fibrinogen the flexibility necessary to diffuse freely in a volume of buffer, only restricted by the dynamic length of the spacer.[27−29] With this cross-linker, the binding sites on the fibrinogen molecule are reachable and the bond between fibrinogen and its receptor on erythrocytes or platelets can be formed.

The number of fibrinogen molecules bound to the AFM tip is not crucial for the force measurements, provided that we are able to identify single molecule detachments from the characteristic stretching curves before rupture.[17,30,31] However, it may affect the rupture distance measurements obtained with a unique tip. As fibrinogen has several accessible primary amines,[32] its binding site cannot be defined *a priori* and the part of the protein that is exposed for binding may vary from molecule to molecule. This, conjugated with the fact that the membranes of erythrocytes and platelets are very elastic, makes the rupture length values achieved by force spectroscopy for both blood cells not as relevant as the respective rupture forces (*vd.* Figure 3).

On our measurements, platelets are already partially activated. However, as our work is focused in erythrocytes, these cells were just used as a (successful) control or proof of concept, demonstrating that in the erythrocyte studies we are actually measuring fibrinogen−receptor interactions, ruling out any type of artifact.

The validation of the association of the forces determined with certain molecular recognition events is a key issue for all force spectroscopy studies. This is especially relevant when we are measuring the interaction of a molecule on the AFM tip with an entire living cell, instead of a purified molecule attached to the substrate. In the present study, this validation was thoroughly conducted based on the well characterized interaction of fibrinogen with its receptor on the platelets membrane and through the theoretically expected substantial decreases on the fibrinogen-platelet interactions observed experimentally: (i) in the absence of $Ca^{2+}$; (ii) in the presence of eptifibatide; and (iii) for a Glanzmann thrombasthenian patient (all discussed below). To conclude if the binding between fibrinogen and erythrocytes could be through an integrin $\alpha_{IIb}\beta_3$-related receptor, we performed the same force spectroscopy experiments with erythrocytes changing the same specific experimental conditions.

As a negative control for our study, we collected cells from one patient with Glanzmann thrombasthenia who, as shown by the genetic analysis, presents a pathogenic mutation in the *ITGB3* gene, which was previously described as causing Glanzmann thrombasthenia.[33] This mutation leads to a nonfunctional expression of the glycoprotein $\alpha_{IIb}\beta_3$ platelet receptor.[33,34] From the force spectroscopy results, we could see that the force necessary to break the bond between fibrinogen and platelets decreases 61% and for the fibrinogen−erythrocyte system it decreases 53%.

As indicated above, the specificity of this fibrinogen−cell binding was also confirmed using calcium depletion as a negative control. The role of divalent cations in integrin function is thoroughly demon-

strated in the literature by the lack of ligand binding upon their removal by chelating agents.[35] Fibrinogen binding to the $\alpha_{IIb}\beta_3$ receptor requires $Ca^{2+}$ to activate the integrin complex.[5] In our study, we could conclude that the effect of the absence of calcium is more significant for the fibrinogen-platelet system than for erythrocytes. The presence of calcium ions emerged to be crucial for a strong binding between platelets and fibrinogen, as expected. In the presence of EDTA 1 mM, the existence of traces of $Ca^{2+}$ in solution appears to be sufficient for a certain level of binding to occur. However, by increasing EDTA concentration to 4 mM, the fibrinogen−erythrocyte interaction decreases dramatically to values similar to those obtained for the platelet-fibrinogen system. The loss of fibrinogen specific binding caused by the cation chelator suggests the involvement of an integrin-type receptor in the fibrinogen−erythrocyte interaction. This integrin would not be as calcium dependent as the platelet receptor.

We also analyzed the effect of the presence of a specific inhibitor of the glycoprotein $\alpha_{IIb}\beta_3$ platelet receptor, eptifibatide, commonly administrated in hospital settings to patients with acute coronary syndromes in order to minimize platelet aggregation, coronary thrombosis and angina, among other vascular conditions.[7,36] The eptifibatide concentrations tested in this study are in accordance with those previously used to test the efficacy of this compound and with the doses administered to patients.[7,36] All the eptifibatide concentrations used significantly inhibit the binding between fibrinogen and platelets, as expected. The few binding/unbinding events detected in the presence of eptifibatide present weak rupture forces. A complete inhibition would not be expected, due to eptifibatide's reversible effect, low affinity to glycoprotein $\alpha_{IIb}\beta_3$ receptor ($K_d$ = 15 nM) and rapid platelet dissociation time.[7,36] Results with erythrocytes show that their interaction with fibrinogen is also inhibited by eptifibatide, but with a lower efficiency.

It is known that several integrin and nonintegrin receptors may bind to known recognition sites on human fibrinogen and regulate some cell functions (*e.g.*, adhesion, aggregation, migration and proliferation).[3] The existence of integrin $\alpha_{IIb}\beta_3$ on erythrocytes is controversial. Some authors reported the existence of this receptor and the nonintegrin glycoprotein Ib,[37] other authors contradicted these results.[38] There were also several reports showing the involvement of integrin and nonintegrin glycoproteins in erythrocytes adhesion to endothelial cells.[37,39,40]

Our results indicate that an integrin receptor is involved in the fibrinogen specific binding to erythrocyte membranes. This receptor is not as calcium dependent and as influenced by the presence of eptifibatide as the glycoprotein $\alpha_{IIb}\beta_3$ platelet receptor; however, its inhibition by eptifibatide indicates that the receptor for fibrinogen on erythrocytes is not the glycoprotein $\alpha_{IIb}\beta_3$, but a related integrin. The results obtained for the Glanzmann thrombastenia patient show for the first time that in this hereditary disease the binding of fibrinogen to erythrocytes is also impaired. The correlation of the force spectroscopy data with the genetic sequencing demonstrates that one of the units of the integrin receptor for fibrinogen on erythrocytes is also a product of the expression of the $\beta_3$ gene (*ITGB3*), found to be mutated in this patient.

Furthermore, our results clearly demonstrate the AFM force spectroscopy technique applicability as a highly sensitive, rapid and low operation cost nanotool for the diagnostic of hematological disorders, using blood cells from patients with genetic mutations. This methodology enables a unique unbiased functional nanodiagnostic (at the single-molecule level) of the severity of the disease for Glanzmann thrombastenia patients.

## METHODS

**Blood Cells Isolation.** Blood was collected from adult donors into $K_3$EDTA anticoagulant tubes. Blood from healthy blood donors was obtained with their previous written informed consent, following a protocol with the Portuguese Blood Institute (Lisbon, Portugal). Blood from the Glanzmann thrombasthenia patient was obtained with her previous written informed consent in the Immune-Hemotherapy Service from the Santa Maria Hospital (Lisbon, Portugal). For the AFM experiments, blood cells were centrifuged at 1040× *g* for 10 min in a Sorvall TC6 centrifuge and washed three times with buffered saline glucose citrate (BSGC; 1.6 mM $KH_2PO_4$, 8.6 mM $Na_2HPO_4$, 0.12 M NaCl, 13.6 mM sodium citrate, 11.1 mM glucose, pH 7.3) supplemented with calcium chloride 1 mM. Erythrocyte final suspensions were prepared with the addition of BSGC buffer, to reconstitute the initial hematocrit (Ht, approximately 45%).

Platelets were isolated from platelet-rich plasma (PRP). Briefly, PRP was separated by centrifugations at 220× *g* for 7 min, at 10 °C. Platelets were pelleted from PRP at 1620× *g* for 10 min, at 10 °C, and washed three times with BSGC buffer with calcium chloride 1 mM. The final pellet was ressuspended in 1 mL of BSGC buffer and kept at 4 °C before use. Platelets were counted using a Cell-Dyn 1600 (Abbott, Abbott Park, Illinois).

For the atomic force microscopy studies, the erythrocytes were diluted 1/1000 and platelets to 10,000 cells/μL with the BSGC buffer + $CaCl_2$ 1 mM.

The study was approved by the joint Ethical Committee of the Santa Maria Hospital and Faculty of Medicine of the University of Lisbon.

**Blood Cells Deposition.** Five-hundred microliters of platelets or erythrocytes suspension were placed on a clean poly-L-lysine-coated glass slide surface and allowed to deposit for 1 h. Nonadherent cells were removed by 5 sequential dilutions with BSGC buffer + $CaCl_2$ 1 mM, loaded into the AFM and allowed to equilibrate in this buffer for 15 min before force spectroscopy measurements. For AFM imaging, the cells samples were washed with buffer and allowed to dry on air at room temperature. No cell fixation was involved in sample preparation.

**AFM Scanning Images of Human Blood Cells.** A NanoWizard II atomic force microscope (JPK Instruments, Berlin, Germany) mounted on the top of an Axiovert 200 inverted optical microscope (Carl

Zeiss, Jena, Germany) was used for imaging and force spectroscopy experiments. The AFM head is equipped with a 15-μm z-range linearized piezoelectric scanner and an infrared laser.

Imaging of platelets and erythrocytes was performed in air in tapping mode. Oxidized sharpened silicon tips with a tip radius of 6 nm, resonant frequency of about 60 kHz and spring constant of 3 N/m were used for the imaging. Imaging parameters were adjusted to minimize the force applied on the scanning of the topography of the cells. Scanning speed was optimized to 0.3 Hz and acquisition points were 512 × 512. Imaging data were analyzed with the JPK image processing v.3 (JPK Instruments, Berlin, Germany).

**Fibrinogen-AFM Tips Functionalization.** For the functionalization, AFM silicon nitride tips were cleaned with an intense ultraviolet light source and silanized in a vacuum chamber with 3-aminopropyl-triethoxysilane (APTES, 30 μL) and *N*,*N*-diisopropylethylamine (10 μL) for 1 h in an argon atmosphere, to be coated with a self-assembled monolayer of amines. After 1 h, the probes were rinsed with fresh chloroform and dried in nitrogen gas. The amine-terminated AFM probes were then placed in glutaraldehyde solution 2.5% (v/v) for 20 min and washed 3 times with PBS (phosphate buffered saline) pH 7.4. Finally, the tips were placed in a fibrinogen solution to attach the fibrinogen molecules to the AFM tip. Purified human fibrinogen (Sigma Aldrich Co, St. Louis, Missouri) was used at a concentration of 1 mg/mL on a 30 min incubation.[28,41] The functionalized fibrinogen tips were immediately mounted on the AFM and used for the force spectroscopy experiments.

**Force Spectroscopy on an Atomic Force Microscope.** Force spectroscopy measurements were performed using fibrinogen functionalized OMCL TR-400-type silicon nitride tips (Olympus, Tokyo, Japan). The softest triangular cantilevers, with a tip radius of 15 nm and a resonant frequency of 11 kHz, were used. The spring constants of the tips were calibrated by the thermal fluctuation method, resulting in values of 0.019 ± 0.007 N/m. For every contact between cell and cantilever, the distance between the cantilever and the cell was adjusted to maintain an applied force of 1 nN before retraction. Molecular recognition was searched by intermittently pressing the cantilevers on different points of the cells adsorbed on the glass slide. Data collection for each force−distance cycle was performed at 2 μm/s, leading to a loading rate of 4 nN/s. To extract kinetic bond rupture parameters, using the Bell, Evans and Ritchie model,[19,20] AFM dynamic force spectra were performed for the two fibrinogen-blood cell receptor interactions. Force curves were analyzed using the JPK image processing v.3 (JPK Instruments, Berlin, Germany). For any given experiment, approximately 8000 force−distance curves were collected, analyzed and fitted to the worm-like-chain model (WLC).[42] Each experiment was performed at least three times, each time on different samples and with different functionalized tips. Histograms of the unbinding forces of each studied fibrinogen-cell complex were constructed choosing the ideal bin size to achieve the best fitted Gaussian model peak forces. Selected binning sizes consistently ranged between 14 and 16 pN. Force rupture values ranging between 0 and 10 pN were considered to represent noise, artifacts or nonspecific interactions. According to this, the values up to 10 pN were neglected in data presentation and analysis. From each histogram, the most likely single fibrinogen molecule rupture force can be determined by fitting the distributions of the rupture forces with the Gaussian model. The maximum values of the Gaussian peaks represent a single-molecule-based statistical measure of the strength of the molecular bond.

**Force Spectroscopy at Different Calcium Concentrations.** To study the influence of the presence of calcium ions, we performed identical force spectroscopy measurements, but with buffered saline glucose citrate (BSGC) buffer without calcium chloride $CaCl_2$ and with ethylenediamine tetraacetic acid (EDTA, a calcium ions chelator). Two different EDTA concentrations were used (1 mM and 4 mM). This new buffer was used on the blood cells isolation processes and on the AFM measurements, as described above.

**Force Spectroscopy at Different Eptifibatide Concentrations.** Eptifibatide (a kind gift from GlaxoSmithKline plc, U.K.) is a reversible inhibitor of fibrinogen binding to the $\alpha_{IIb}\beta_3$ receptor in platelets, and is one of the identified drugs that reduce blood clotting. It is clinically used for the treatment of undesired increased platelet aggregation upon different vascular pathologic conditions.[7,36] To analyze the effect of the addition of different eptifibatide concentrations on the binding between fibrinogen and erythrocytes or platelets, blood cells were isolated as described above, with BSGC buffer + $CaCl_2$ 1 mM. After removing non adherent cells, similar erythrocytes/platelets aliquots were incubated for 45 min with increasing concentrations of eptifibatide (3.4, 8.5, and 17 μg/mL; 4−20 μM) at room temperature. Force spectroscopy experiments were carried out in the presence of each eptifibatide concentration.

**AFM Additional Control Experiments.** All the interactions between fibrinogen and blood cells were studied at room temperature in physiological buffer (BSGC). The AFM laboratory is strictly maintained between 23 and 25 °C. Small variations in temperature on this range did not affect the force spectroscopy measurements, even after a long period of experiment. The same percentage of cell-fibrinogen (un)binding events and rupture force values were obtained at the end of the day-long experiments.

As controls for tip modification, measurements with tips at the different steps of their functionalization process (including nonfunctionalized tips) were conducted on glass slides, with and without poly-L-lysine, and on blood cells.

**Genetic Analysis.** The patient's genomic DNA was extracted from a peripheral blood sample using standard procedures. The *ITGA2B* and the *ITGB3* genes, which are associated with Glanzmann thrombasthenia due to the expression of the $\alpha_{IIb}$ and $\beta_3$ subunits, respectively, were investigated for mutations. Intronic primers were designed to flank each of the 30 *ITGA2B* and 15 *ITGB3* exons (GenBank accession number NM_000419 for *ITGA2B* and NM_000212 for *ITGB3*). Primer sequences are available upon request. Polymerase chain reactions (PCR) were performed in a 25 μL reaction volume, using 10 μM of each primer, 2.5 μL of 10× reaction buffer [160 mM $(NH_4)_2SO_4$, 670 mM Tris-HCl pH 8.8, 0.1% Tween-20] (Bioline, London, UK), 1.5 mM $MgCl_2$, 0.2 mM dNTPs and 1 U of BioTaq polymerase (Bioline, London, UK).

An 100 ng aliquot of genomic DNA was denatured for 5 min at 94 °C, followed by 30 cycles of amplification (45 s at 95 °C; 45 s at specific annealing temperature; 45 s at 72 °C) followed by a 10 min extension at 72 °C. PCR products were tested on a 2% agarose gel. After purification, the PCR products were sequenced on an automated sequencer ABI PRISMR 3100-Avant using a BigDye v3.1 sequence kit (Applied Biosystems, Carlsbad, California). Sequencing analysis was done in both strands of the PCR amplified exons whenever a mutation was found. Nucleotide numbering for *ITGA2B* is according to the cDNA nucleotide sequence of Poncz *et al.*[43] and for *ITGB3* according to the nucleotide sequence of Fitzgerald *et al.*[44] Modifications for the nomenclature of the mutations are according to the international GT mutation database (http://sinaicentral.mssm.edu/intranet/research/glanzmann/play?page=nomenclature).

*Acknowledgment.* We thank Mrs. T. Freitas (Faculdade de Medicina da Universidade de Lisboa) for excellent technical assistance and GlaxoSmithKline plc. for the kind gift of eptifibatide. This work was supported by Fundação para a Ciência e a Tecnologia−Ministério da Ciência, Tecnologia e Ensino Superior (FCT-MCTES, Portugal; grants CONC-REEQ/140/2001 and PTDC/SAU-OSM/73449/2006) and by Fundação Calouste Gulbenkian (Portugal).

## REFERENCES AND NOTES

1. Cross, S. E.; Jin, Y. S.; Rao, J.; Gimzewski, J. K. Nanomechanical Analysis of Cells from Cancer Patients. *Nat. Nanotechnol.* **2007**, *2*, 780–783.
2. Aigner, T.; Schmitz, N.; Haag, J. Nanomedicine: AFM Tackles Osteoarthritis. *Nat. Nanotechnol.* **2009**, *4*, 144–145.
3. Herrick, S.; Blanc-Brude, O.; Gray, A.; Laurent, G. Fibrinogen. *Int. J. Biochem. Cell Biol.* **1999**, *31*, 741–746.
4. Plow, E. F.; Haas, T. A.; Zhang, L.; Loftus, J.; Smith, J. W. Ligand Binding to Integrins. *J. Biol. Chem.* **2000**, *275*, 21785–21788.
5. Bennett, J. S. Structure and Function of the Platelet Integrin $\alpha_{IIb}\beta_3$. *J. Clin. Invest.* **2005**, *115*, 3363–3369.

6. Lee, I.; Marchant, R. E. Molecular Interaction Studies of Hemostasis: Fibrinogen Ligand-Human Platelet Receptor Interactions. *Ultramicroscopy* **2003**, *97*, 341–352.
7. Holmes, M. B.; Sobel, B. E.; Schneider, D. J. Variable Responses to Inhibition of Fibrinogen Binding Induced by Tirofiban and Eptifibatide in Blood from Healthy Subjects. *Am. J. Cardiol.* **1999**, *84*, 203–207.
8. Nurden, A. T.; Poujol, C.; Durrieu-Jais, C.; Nurden, P. Platelet Glycoprotein IIb/IIIa Inhibitors: Basic and Clinical Aspects. *Arterioscler. Thromb. Vasc. Biol.* **1999**, *19*, 2835–2840.
9. Lim, B. B.; Lee, E. H.; Sotomayor, M.; Schulten, K. Molecular Basis of Fibrin Clot Elasticity. *Structure* **2008**, *16*, 449–459.
10. Nurden, A. T. Glanzmann Thrombasthenia. *Orphanet. J. Rare Dis.* **2006**, *1*, 10.
11. George, J. N.; Caen, J. P.; Nurden, A. T. Glanzmann's Thrombasthenia: The Spectrum of Clinical Disease. *Blood* **1990**, *75*, 1383–1395.
12. Maeda, N.; Seike, M.; Kume, S.; Takaku, T.; Shiga, T. Fibrinogen-Induced Erythrocyte Aggregation: Erythrocyte-Binding Site in the Fibrinogen Molecule. *Biochim. Biophys. Acta* **1987**, *904*, 81–91.
13. Delamaire, M.; Durand, F. Erythrocyte Aggregation and Vascular Pathology. *J. Mal. Vasc.* **1990**, *15*, 344–345.
14. Lominadze, D.; Schuschke, D. A.; Joshua, I. G.; Dean, W. L. Increased Ability of Erythrocytes to Aggregate in Spontaneously Hypertensive Rats. *Clin. Exp. Hypertens.* **2002**, *24*, 397–406.
15. Litvinov, R. I.; Bennett, J. S.; Weisel, J. W.; Shuman, H. Multi-Step Fibrinogen Binding to the Integrin $\alpha_{IIb}\beta_3$ Detected Using Force Spectroscopy. *Biophys. J.* **2005**, *89*, 2824–34.
16. Lekka, M.; Fornal, M.; Pyka-Fosciak, G.; Lebed, K.; Wizner, B.; Grodzicki, T.; Styczen, J. Erythrocyte Stiffness Probed Using Atomic Force Microscope. *Biorheology* **2005**, *42*, 307–317.
17. Brown, A. E.; Litvinov, R. I.; Discher, D. E.; Weisel, J. W. Forced Unfolding of Coiled-Coils in Fibrinogen by Single-Molecule AFM. *Biophys. J.* **2007**, *92*, L39–41.
18. Lominadze, D.; Dean, W. L. Involvement of Fibrinogen Specific Binding in Erythrocyte Aggregation. *FEBS Lett.* **2002**, *517*, 41–44.
19. Bell, G. I. Models for the Specific Adhesion of Cells to Cells. *Science* **1978**, *200*, 618–627.
20. Evans, E.; Ritchie, K. Dynamic Strength of Molecular Adhesion Bonds. *Biophys. J.* **1997**, *72*, 1541–1555.
21. Lee, C. K.; Wang, Y. M.; Huang, L. S.; Lin, S. Atomic Force Microscopy: Determination of Unbinding Force, Off Rate and Energy Barrier for Protein-Ligand Interaction. *Micron* **2007**, *38*, 446–461.
22. Goel, M. S.; Diamond, S. L. Adhesion of Normal Erythrocytes at Depressed Venous Shear Rates to Activated Neutrophils, Activated Platelets, and Fibrin Polymerized from Plasma. *Blood* **2002**, *100*, 3797–3803.
23. Vinciguerra, C.; Trzeciak, M. C.; Philippe, N.; Frappaz, D.; Reynaud, J.; Dechavanne, M.; Negrier, C. Molecular Study of Glanzmann Thrombasthenia in 3 Patients Issued from 2 Different Families. *Thromb. Haemost.* **1995**, *74*, 822–827.
24. Rampling, M. W. The Binding of Fibrinogen and Fibrinogen Degradation Products to the Erythrocyte Membrane and Its Relationship to Haemorheology. *Acta Biol. Med. Ger.* **1981**, *40*, 373–378.
25. Muller, D. J. AFM: A Nanotool in Membrane Biology. *Biochemistry* **2008**, *47*, 7986–7998.
26. Santos, N. C.; Castanho, M. A. An Overview of the Biophysical Applications of Atomic Force Microscopy. *Biophys. Chem.* **2004**, *107*, 133–149.
27. Willemsen, O. H.; Snel, M. M.; Cambi, A.; Greve, J.; De Grooth, B. G.; Figdor, C. G. Biomolecular Interactions Measured by Atomic Force Microscopy. *Biophys. J.* **2000**, *79*, 3267–3281.
28. Chtcheglova, L. A.; Haeberli, A.; Dietler, G. Force Spectroscopy of the Fibrin(ogen)-Fibrinogen Interaction. *Biopolymers* **2008**, *89*, 292–301.
29. de Odrowaz Piramowicz, M.; Czuba, P.; Targosz, M.; Burda, K.; Szymonski, M. Dynamic Force Measurements of Avidin-Biotin and Streptavdin-Biotin Interactions Using AFM. *Acta Biochim. Pol.* **2006**, *53*, 93–100.
30. Tsapikouni, T. S.; Missirlis, Y. F. Measuring the Force of Single Protein Molecule Detachment from Surfaces with AFM. *Colloids Surf., B* **2010**, *75*, 252–259.
31. Francius, G.; Alsteens, D.; Dupres, V.; Lebeer, S.; De Keersmaecker, S.; Vanderleyden, J.; Gruber, H. J.; Dufrene, Y. F. Stretching Polysaccharides on Live Cells Using Single Molecule Force Spectroscopy. *Nat. Protoc.* **2009**, *4*, 939–946.
32. Doolittle, R. F. A Detailed Consideration of a Principal Domain of Vertebrate Fibrinogen and Its Relatives. *Protein Sci.* **1992**, *1*, 1563–1577.
33. Kannan, M.; Ahmad, F.; Yadav, B. K.; Kumar, R.; Choudhry, V. P.; Saxena, R. Molecular Defects in ITGA2B and ITGB3 Genes in Patients with Glanzmann's Thrombasthenia. *J. Thromb. Haemost.* **2009**, *7*, 1878–1885.
34. French, D. L.; Seligsohn, U. Platelet Glycoprotein IIb/IIIa Receptors and Glanzmann's Thrombasthenia. *Arterioscler. Thromb. Vasc. Biol.* **2000**, *20*, 607–610.
35. Fernandez, C.; Clark, K.; Burrows, L.; Schofield, N. R.; Humphries, M. J. Regulation of the Extracellular Ligand Binding Activity of Integrins. *Front. Biosci.* **1998**, *3*, d684–700.
36. Katori, N.; Szlam, F.; Levy, J. H.; Tanaka, K. A. A Novel Method to Assess Platelet Inhibition by Eptifibatide with Thrombelastograph. *Anesth. Analg.* **2004**, *99*, 1794–1799.
37. Wick, T. M.; Moake, J. L.; Udden, M. M.; McIntire, L. V. Unusually Large Von Willebrand Factor Multimers Preferentially Promote Young Sickle and Nonsickle Erythrocyte Adhesion to Endothelial Cells. *Am. J. Hematol.* **1993**, *42*, 284–292.
38. Joneckis, C. C.; Ackley, R. L.; Orringer, E. P.; Wayner, E. A.; Parise, L. V. Integrin $\alpha_4\beta_1$ and glycoprotein IV (CD36) are expressed on Circulating Reticulocytes in Sickle Cell Anemia. *Blood* **1993**, *82*, 3548–3555.
39. Manodori, A. B. Sickle Erythrocytes Adhere to Fibronectin-Thrombospondin-Integrin Complexes Exposed by Thrombin-Induced Endothelial Cell Contraction. *Microvasc. Res.* **2001**, *61*, 263–274.
40. Sugihara, K.; Sugihara, T.; Mohandas, N.; Hebbel, R. P. Thrombospondin Mediates Adherence of $CD36^+$ Sickle Reticulocytes to Endothelial Cells. *Blood* **1992**, *80*, 2634–2642.
41. Barattin, R.; Voyer, N. Chemical Modifications of AFM Tips for the Study of Molecular Recognition Events. *Chem. Commun.* **2008**, 1513–1532.
42. Ratto, T. V.; Rudd, R. E.; Langry, K. C.; Balhorn, R. L.; McElfresh, M. W. Nonlinearly Additive Forces in Multivalent Ligand Binding to a Single Protein Revealed with Force Spectroscopy. *Langmuir* **2006**, *22*, 1749–1757.
43. Poncz, M.; Eisman, R.; Heidenreich, R.; Silver, S. M.; Vilaire, G.; Surrey, S.; Schwartz, E.; Bennett, J. S. Structure of the Platelet Membrane Glycoprotein IIb. Homology to the $\alpha$ Subunits of the Vitronectin and Fibronectin Membrane Receptors. *J. Biol. Chem.* **1987**, *262*, 8476–8482.
44. Fitzgerald, L. A.; Steiner, B.; Rall, S. C., Jr.; Lo, S. S.; Phillips, D. R. Protein Sequence of Endothelial Glycoprotein IIIa Derived from a cDNA Clone. Identity with Platelet Glycoprotein IIIa and Similarity to "Integrin". *J. Biol. Chem.* **1987**, *262*, 3936–3939.